ELSEVIER

Biochimica et Biophysica Acta 1196 (1994) 181–190

BBA Biochimica et Biophysica Acta

Transmembrane potentials in cells: a diS-$C_3(3)$ assay for relative potentials as an indicator of real changes

Jaromír Plášek [a,*], Robert E. Dale [b], Karel Sigler [c], Gábor Laskay [b,1]

[a] *Institute of Physics of the Charles University, Ke Karlovu 5, 121 16 Prague, Czech Republic*
[b] *Cancer Research Campaign Biophysics Research Section, Paterson Institute for Cancer Research, Christie Hospital NHS Trust, Manchester M20 9BX, UK*
[c] *Institute of Microbiology, Czech Academy of Sciences, Vídeňská 1083, 142 20 Prague, Czech Republic*

Received 15 August 1994

Abstract

The mechanism by which the fluorescent cationic dye diS-$C_3(3)$ reports on cellular transmembrane potential has been investigated in murine haemopoietic cells. Due to the large molar absorbance of diS-$C_3(3)$ and its high quantum yield of fluorescence in cells, this dye can be used at very low labelling concentrations ($5 \cdot 10^{-8}$ to $2 \cdot 10^{-7}$ M). In contrast to the quenching of fluorescence observed for the most commonly used voltage-sensitive dyes of the carbocyanine class, the fluorescence intensity of diS-$C_3(3)$ increases when the dye accumulates in the cells. The method of synchronous emission spectroscopy was used to resolve the intracellular and extracellular components of the diS-$C_3(3)$ fluorescence of suspensions of labelled cells. In comparing changes in these signals consequent on changes in transmembrane potential induced by varying the extracellular concentration of potassium ions in the presence of valinomycin, the logarithm of the ratio of intensities of these two components, as predicted theoretically, was found to be a good linear measure of transmembrane potential under these conditions. The dye was also demonstrated to be suitable for flow-cytofluorimetric analysis, the logarithm of the mean population signal similarly being found to provide a good linear measure of the transmembrane potential. The conditions under which such linearity may be expected with respect to possible effects due to changes in the capacity for binding of the dye to proteins and various cytosolic structures are delineated and their validity with respect to the possibly contentious role of mitochondria in such measurements examined in particular. The use of the method in indicating changes in the transmembrane potential and/or changes in the transport numbers of the major ions determining transmembrane potential between different physiological states, the possible extension to determinations of *absolute* differences in potential between different cell states without calibration or comparison with potassium-ion potentials, and the conditions for validity and limitations of these partially complementary measurements, are discussed.

Keywords: Transmembrane potential; DiS-$C_3(3)$; 3,3′-Dipropylthiacarbocyanine; Spectral analysis; Flow cytometry; Confocal microscopy

1. Introduction

Over the past two decades, several efficient fluorescent indicators of cell transmembrane potential have been developed and used in numerous studies on living cells (for reviews see, e.g., [1–7]). This report deals with photophysical and potentiometric properties of 3,3′-dipropylthiacarbocyanine, diS-$C_3(3)$, the 'forgotten' member of the thiacarbocyanine family of slow (accumulation, or redistribution) fluorescent transmembrane potential indicators.

The slow dyes monitor transmembrane potential by their voltage-dependent partition between the extracellular medium and the cytosol. Equilibrium concentration gradients of such redistribution dyes obey the Nernst equation. Cell hyperpolarization will therefore be reflected in an increased free intracellular cationic dye concentration, i.e., by accumulation of the dye in cells, and, vice-versa, a decreased accumulation will reflect depolarization [8–10]. A voltage-dependent partition of thiacarbocyanine dyes from aqueous solutions into lipid bilayers has also been observed [11,12], but this is unlikely to contribute considerably to the overall rate of dye accumulation in whole

* Corresponding author. E-mail: plasek@karlov.mff.cuni.cz. Fax: +42 11 268199.

[1] Permanent address: MTA Group, Department of Botany, József Attila University, Egyetem u. 2, H-6722 Szeged, Hungary.

SSDI 0005-2736(94)00209-6

cells, since the volume of cell membranes is negligible compared to the total cell volume and no accumulation of highly fluorescent dye into the plasma membrane of these cells is evident under the microscope (see also Fig. 7 below).

The accumulation of a fluorescent probe in cells is usually assessed by monitoring its fluorescence intensity. In the case of diS-C_3(5), which turned out to be a prototype for the thiacarbocyanine group [8], the hyperpolarization of cells is monitored as a pronounced decrease in fluorescence intensity. This decrease results from the formation of non-fluorescent dimers and/or higher aggregates of the probe molecules upon their accumulation in cells [8,9,13]. However, some of the internalized dye is also bound to proteins or other cytosolic components [14]. For diS-C_3(5), despite the overall quenching of fluorescence observed, such binding is manifested by the existence of a definite new spectral component in its fluorescence, shifted by about 17 nm to the red [15] as compared to the fluorescence in aqueous solutions.

The above overall pattern of fluorescence changes following dye partition into cells does not hold for diS-C_3(3), however. Originally presented by Peña and co-workers as a good qualitative indicator of transmembrane potential in yeasts, diS-C_3(3) reports its accumulation in cells by *increased* fluorescence intensity [16]. Consequently this dye has long been ignored as giving results incompatible with the popular diS-C_3(5) assays.

A critical problem in the probing of cell transmembrane potential with any redistribution probe is the calibration of probe response in terms of absolute potential differences across the membrane. This is usually accomplished by valinomycin clamping of transmembrane potential at defined potassium gradients [9,10,13,17]. No proof is usually available, however, that the main assumptions of the calibration procedure (that valinomycin enables the establishment of an equilibrium potassium potential, and/or that the true intracellular potassium concentration needed to calculate it is known) are valid.

Even apart from problems relating to the calibration procedure per se, the assessment of transmembrane potential with thiacarbocyanine dyes may not be unequivocal. Since these dyes accumulate in cells, their toxicity is often not negligible, particularly at the high labelling concentrations necessary with diS-C_3(5). Moreover, certain other artifactual changes in transmembrane potential may also take place as a result of too high a dye accumulation in the cells [2,5,18,19]. Unfortunately, the extent of diS-C_3(5) accumulation in cells cannot easily be minimized without compromising the accuracy of measurement of fluorescence intensity of the sample: the dye concentration within the relatively small volume of cells (typically of the order of 10^{-4} to 10^{-3} of the total volume of the suspension) must obviously be very high in order to achieve a substantial decrease of the fluorescence intensity in the suspension as a whole.

Last, but not least, dyes such as diS-C_3(5) are not suitable for the analysis of transmembrane potential in individual cells by flow cytometry and microfluorimetry since their fluorescence is quenched upon their accumulation in cells. For this purpose, a dye that increases its fluorescence on accumulation within cells, such as the rarely used thiacarbocyanine dye, diS-C_3(3), should be more appropriate. All of the data on transmembrane potential-reporting properties of this dye presented here were obtained with murine haemopoietic cells, as a part of wider project on membrane-related changes elicited by the action of the specific growth factor interleukin-3 (IL-3).

2. Materials and methods

2.1. Chemicals

DiS-C_3(3) was purchased from Molecular Probes (USA), valinomycin, Hepes, and bovine serum albumin from Sigma (UK), other common chemicals from Aldrich (UK).

2.2. Cell culture

Murine haemopoietic cells (cell line FDCP-Mix, clone A4 [20]) were cultured in Fischer's medium supplemented with 20% horse serum and 1% murine interleukin-3 (IL-3) conditioned medium as the growth factor source. The cells were maintained in a logarithmic phase of population growth by subculturing every third day into fresh media. Before transmembrane potential assays, cell viability was assessed by the Trypan blue exclusion test: the cell viability thus measured was typically 90–95%.

2.3. Cell labelling

Cells were washed twice in Hepes buffer (5 mM, pH 7.4) containing defined concentrations of KCl and NaCl (see below), and resuspended to a final concentration of $(1–6) \cdot 10^6$ cells/ml. Aliquots of such suspensions were labelled with dye at a final concentration between $2 \cdot 10^{-8}$ and $6 \cdot 10^{-6}$ M. The dye was added as a stock solution in ethanol (10^{-4} or 10^{-3} M) in such a way that the final ethanol concentration did not exceed 0.5% (v/v), following which fluorescence spectra were measured after a 5 minute equilibration period during which the suspension was gently mixed to ensure as uniform labelling as possible.

2.4. Fluorescence measurements

Fluorescence spectra were measured with a Shimadzu RF-540 spectrofluorimeter. The determination of synchronous emission spectra (SES) proved to be an efficient

tool for spectroscopic discrimination between free diS-$C_3(5)$ dye in buffer and its bound form in cells [15]. SES spectra (measured by simultaneous scanning of both fluorescence excitation and emission wavelengths, keeping the wavelength difference between them constant [21–23]) were recorded over the emission wavelength range from 520 to 620 nm, with the excitation-emission wavelength difference ($\Delta\lambda_{SES}$) set at 12.5 nm and bandwidths of 5 nm in both excitation and observation. The spectra presented here are corrected neither for the spectral distribution of excitation light intensity, nor for the spectral sensitivity of the detection system.

2.5. Analysis of SES spectra

As shown below, diS-$C_3(3)$ exhibits fluorescence spectral changes both on binding to albumin and on redistributing from the extracellular medium into cells, the latter presumably due largely to the binding of dye to cytosolic proteins. If it is assumed that two distinct dye forms coexist in these cases (cell suspensions and albumin solutions), i.e., the free (aqueous) and protein-bound forms, then experimental synchronous emission spectra, $F_c(\lambda)$, in such samples can be expressed in terms of the linear combination:

$$F_c(\lambda) = aF_a(\lambda) + bF_b(\lambda) \quad (1)$$

where $F_a(\lambda)$ and $F_b(\lambda)$ are the peak-height normalized synchronous emission spectra of free and bound forms of the dye, respectively, a and b the corresponding fractions of these spectra in the overall spectrum $F_c(\lambda)$. In view of the low relative volume of cells in suspensions (less than $1.5 \cdot 10^{-3}$ of the total), the fluorescence of unbound dye within cells is assumed to contribute negligibly to the calculated aF_a component.

The linear decomposition of experimental spectra was based on least-squares fitting. For this purpose, the normalized SES of diS-$C_3(3)$ in Hepes was used as F_a. The model F_b spectrum was obtained by measuring several probe SES, both in suspensions of hyperpolarized cells and in 2% aqueous albumin solutions. Their aF_a components were estimated empirically by scaling the F_a spectrum with a suitably low coefficient and then subtracting the result from these experimental SES, repeating the procedure several times with increased values of the coefficient until part of the resultant difference spectrum became zero. The procedure is schematically illustrated in Fig. 1. The average of these empirical difference SES weighted by the inverse of the coefficient b (i.e., after peak normalization) was determined and taken as the model F_b. Further experimental spectra were analyzed by adjusting the coefficients a and b in Eq. (1) to obtain the minimum sum of squares of differences between the sum of the fractional model F_a and F_b spectra and the experimental F_c.

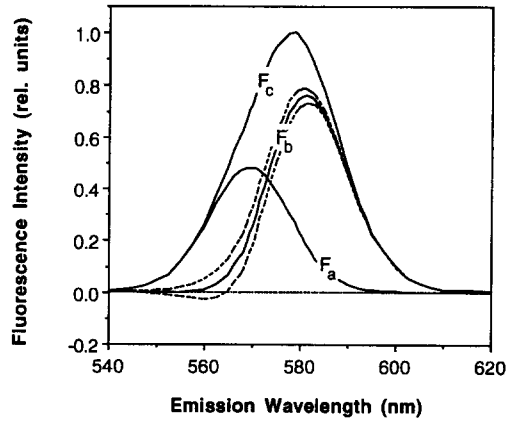

Fig. 1. Spectral decomposition of experimental fluorescence of $3.75 \cdot 10^{-8}$ M diS-$C_3(3)$ in suspensions of $6 \cdot 10^6$ FDCP-Mix clone A4 cells/ml in Hepes containing 5 mM KCl and $1.5 \cdot 10^{-6}$ M valinomycin (pH 7.4). Two distinct spectral components, F_a and F_b in their analysed proportions a and b, respectively, and their sum F_c, the overall measured spectrum, are plotted as full lines. The dotted curves show the results of empirical subtractions of the aF_a components when the estimation of aF_a is too low (upper curve) or too high (lower curve).

2.6. Flow cytometry

The probe emission from cells, essentially bF_b completely separated from the component aF_a in the extracellular medium, was also analyzed using an EPICS V flow-cytometer (Coulter Electronics, USA). The probe was excited with an argon-ion laser (514.5 nm, 200 mW) and its emission detected at 590 nm. Together with the fluorescence intensity of the individual cells, light scattered in the forward direction (1–19°), the intensity of which is roughly proportional to the cross-sectional area of the cell, was also measured.

The observed fluorescence intensity in suspensions of FDCP-Mix clone A4 cells was approximately proportional to this measure of cell size and, as expected from this, the halfwidths (FWHM) of a cell number versus fluorescence intensity histogram were proportional to the mean fluorescence intensity (I_{mean}), which was selected as the most convenient measure of diS-$C_3(3)$ accumulation in cells.

2.7. Theory of the relative transmembrane potential calibration procedure

Under appropriate conditions, the ratio b/a of the synchronous emission spectral intensities of the distributed fluorescent probe is expected to be proportional to the ratio of the corresponding *unbound* dye concentrations inside (c_{in}) and outside (c_{out}) the cell, that is:

$$Q = b/a = Pc_{in}/c_{out} \quad (2)$$

where the coefficient P is the product of the following factors: (i) the relative volume of cells in the suspension, (ii) the ratio of the fluorescence quantum yields of bound and free aqueous dye forms, (iii) the ratio of the concentra-

tion of bound to that of unbound dye within the cells (up to about 10% of saturation of binding), and (iv) spectral variation in the sensitivity of detector.

The ratio of concentrations c_{in} and c_{out} obeys the Nernst equation:

$$c_{in} = c_{out} \exp(-FV/RT) \quad (3)$$

where V is the transmembrane potential. From Eqs. (2) and (3), it follows that an estimate of V is given by:

$$V = -(RT/F)(\ln Q - \ln P) \quad (4)$$

where $\ln P$ is a constant which is difficult, if not impossible, to determine in practice. However, *changes* of transmembrane potential with respect to some arbitrary reference state can be quantified because, in that case, the $\ln P$ term cancels out. Thus, taking for example the transmembrane potential at an extracellular potassium concentration $[K^+]_{out} = 130$ mM as such a reference, a difference of transmembrane potentials ΔV which no longer contains the additive constant can be defined:

$$\Delta V = V - V_{130} = -(RT/F)\ln(Q/Q_{130}) \quad (5)$$

Q_{130} being the value of Q measured at $[K^+]_{out} = 130$ mM. In this way, a scale (directly in mV) for quantitating differences (or changes) of transmembrane potential with respect to a certain arbitrary reference state has, in principle, been constructed, while the absolute values remain undetermined.

The situation for the flow-cytometric determinations is a little different. Here the measured fluorescence intensities (I_{mean}) are of the intracellular component essentially completely separated from that in the extracellular medium, i.e., a measure of the average concentration of dye accumulated in the cells, analogous to b, the intensity of bound dye fluorescence in cell suspensions. Since the total amount of dye per unit volume of suspension is constant, Eq. (3) may be expressed in terms of the constant overall concentration of dye (C) and the ratio of cell volume to total volume in the suspension (v):

$$c_{in} = C \exp(-FV/RT)/(1 - v + v \exp(-FV/RT)) \quad (6)$$

For $6 \cdot 10^6$ cells/ml, v will be less than $1.5 \cdot 10^{-3}$ (approximation of spherical cell diameter less than 8 μm). Furthermore, the K^+-dominated transmembrane potential for the minimum external concentration of potassium ion (5 mM), assuming as high as a 250 mM internal concentration, yields a value of 50 for the exponential. Then the value of $v \exp(-FV/RT)$ will certainly be less than 0.1, and probably always less than 0.05. Under these conditions, it may safely be assumed that the analogue of Eq. (5) in which Q/Q_{130} is replaced by $I_{mean}/I_{mean130}$ will hold to a very good approximation:

$$\Delta V = V - V_{130} = -(RT/F)\ln(I_{mean}/I_{mean130}) \quad (7)$$

An equivalent argument for c_{out} shows that it changes very little within the relevant range of transmembrane potential.

Eq. (5) may also be re-expressed as:

$$\Delta V = V - V_{130} = -(RT/F)(\ln(b/b_{130}) - \ln(a/a_{130})) \quad (8)$$

Since a/a_{130} is less than but close to unity, while b/b_{130} can range over much larger or much smaller values, it essentially disappears from Eq. (8), establishing a near equivalence for the SES and flow-cytometric estimates of ΔV.

In general, the bound probe signal from cells may be expected to reflect a superposition of bound probe signals from both cytosol and mitochondria, since the latter are known to exhibit their own transmembrane potential (V_m). The concentration of the dye accumulated in mitochondria (c_m) can again be calculated according to the Nernst equation:

$$c_m = c_{in} \exp(-FV_m/RT) \quad (9)$$

in which c_{in}, the dye concentration in the cytosol, corresponds to that in the extramitochondrial space. On substituting the value of c_{in} given by Eq. (3):

$$c_m = c_{out} \exp(-F(V_m + V)/RT) \quad (10)$$

Allowing for different values of the coefficients P_c and P_m for fluorescence from cytosol and mitochondria, respectively, the total fluorescence intensity from a suspension of cells containing active mitochondria should be well approximated by:

$$Q = b/a = (P_c c_{in} + P_m c_m)/c_{out} \quad (11)$$

and, after substitution of Eqs. (3) and (10) for c_{in} and c_m, respectively:

$$Q = [P_c + P_m \exp(-FV_m/RT)] \exp(-FV/RT) \quad (12)$$

As long as the mitochondrial transmembrane potential remains constant, the value of $[P_c + P_m \exp(-FV_m/RT)]$ is also constant. This constant is again eliminated when the Q/Q_{ref} ratio is calculated. In such a case, therefore, Eq. (5) remains valid also for cells with active mitochondria, and the logarithm of this ratio reflects solely the difference in the plasma membrane potential between the two states, even though b may include a possibly overwhelming contribution from dye bound within mitochondria.

The theoretical value of the potassium ion diffusion potential, V_{K^+}, in cells can also be calculated, according to the Nernst equation:

$$V_{K^+} = -(RT/F)\ln([K^+]_{in}/[K^+]_{out}) \quad (13)$$

where $[K^+]_{in}$, the intracellular potassium concentration, is usually not reliably known. However, since $[K^+]_{in}$ remains essentially constant because only a fraction of about 10^{-5} of the total K^+ is exchanging due to the establishment of any of the Nernst equilibria considered here [24], a relative scale, ΔV_{K^+}, can also be constructed for these theoretical values:

$$\Delta V_{K^+} = V_{K^+} - V_{130} = -(RT/F)\ln(130/[K^+]_{out}) \quad (14)$$

with $[K^+]_{out}$ defined in units of mM.

2.8. Transmembrane potential measurements

The transmembrane potential in valinomycin-clamped FDCP-Mix clone A4 cells was assayed with diS-C_3(3) as a function of extracellular potassium-ion concentration [9,10,13]. Seven KCl concentrations in the Hepes buffer were used (5, 8, 15, 25, 45, 70 and 130 mM), NaCl being added together with the KCl to keep the sum of $[K^+]$ and $[Na^+]$ constant at 150 mM. The valinomycin (10^{-6} M) was added together with the dye after resuspending cells in these media, and samples were labelled as described above. Care was taken to minimize differences in incubation periods for the various samples (5 to 10 min). For each of the different KCl concentrations, the probe SES of the suspensions were analyzed spectroscopically, using Eq. (1), and intracellular probe fluorescence was monitored in the flow-cytometer.

The experimental SES were decomposed into their respective aF_a and bF_b components as described above. The values of a and b obtained for the given extracellular potassium concentrations were then used to construct an apparent calibration curve for relative transmembrane potential. In the case of flow-cytometric analysis the I_{mean} values (equivalent to b) were used for this purpose. All calibration experiments were performed at room temperature, i.e., at 24 ± 2°C, corresponding to RT/F values of 25.6 ± 0.2 mV.

3. Results

3.1. Synchronous emission spectra (SES) of diS-C_3(3) solutions

The emission, excitation and synchronous emission spectra of diS-C_3(3) solutions in four pure solvents of different polarity were measured and the results are summarized in Table 1. The ordinary emission and excitation spectra of diS-C_3(3) fluorescence in Hepes buffer (pH 7.4) are shown in Fig. 2. Based on the difference between the excitation and emission maxima, the wavelength difference

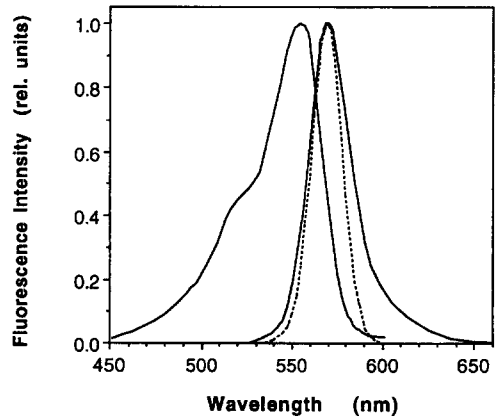

Fig. 2. Fluorescence spectra of $2 \cdot 10^{-6}$ M diS-C_3(3) in Hepes (pH 7.4): excitation spectrum (full line, left), $\lambda_{em} = 615$ nm (bandwidths $\Delta\lambda_{em} = 10$ nm, $\Delta\lambda_{ex} = 2$ nm); emission spectrum (full line, right), $\lambda_{ex} = 505$ nm (bandwidths $\Delta\lambda_{em} = 2$ nm, $\Delta\lambda_{ex} = 10$ nm). Synchronous emission spectrum (SES), (dashed line), $\Delta\lambda_{SES} = \lambda_{em} - \lambda_{ex} = 12.5$ nm (bandwidths $\Delta\lambda_{em} = \Delta\lambda_{ex} = 5$ nm).

for recording the SES was set at 12.5 nm. The SES spectrum of diS-C_3(3) solution in Hepes consists of a single sharp peak with a maximum at $\lambda = 569$ nm. The halfwidth was 19.5 nm, compared with more than twice this value in the normal emission and excitation spectra. No difference was found between the spectra of diS-C_3(3) fluorescence measured in Hepes, phosphate-buffered saline (PBS) and pure water. Furthermore, neither the SES of diS-C_3(3) fluorescence in water, nor its ordinary emission and excitation spectra exhibited any pronounced variation on changing the ionic strength (KCl concentrations between 100 and 300 mM) or pH (in the region of 5 to 9) of the solvent.

The synchronous emission spectra of diS-C_3(3) solutions in organic solvents (ethanol, n-butanol, n-hexane) are shown in Fig. 3. With decreasing solvent polarity, the SES maximum is red-shifted and the fluorescence intensity increases (see Table 1). The charged diS-C_3(3) molecule is practically insoluble in very non-polar solvents. In hexane, therefore, a saturated solution of unknown concentration was used in measuring its very weak fluorescence.

Table 1
Dependence of diS-C_3(3) fluorescence parameters in solution on solvent properties

Solvent	Dielectric constant (see [25])	SES maximum (nm)	SES halfwidth (nm)	Relative emission intensity	Dye concn. (10^{-6} M)
Water	75.8	569	21.0	1.0	1.0
Ethanol	24.3	573	20.5	3.2	1.0
n-Butanol	17.1	576	19.5	5.2	1.0
n-Hexane	1.9	581	19.0	– [a]	– [a]
3 M NaOH		582	19.5	4.1 [b]	1.0
10% BSA		582	19.0	5–5.5 [b]	0.3

[a] Saturated solution of unknown concentration.
[b] Relative intensity determined as the ratio of calculated bF_b values to the concomitant decrease of the aqueous component, aF_a (see text).

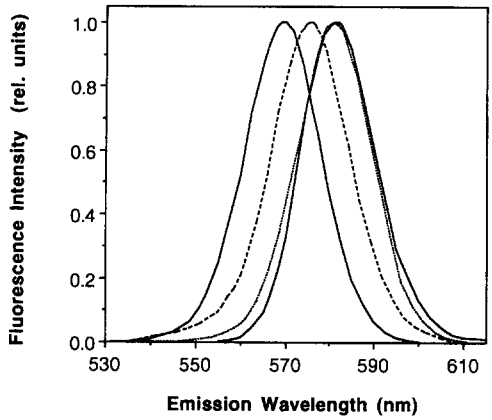

Fig. 3. Synchronous emission spectra of diS-C_3(3) solutions: in Hepes at pH 7.4 ($2 \cdot 10^{-6}$ M dye concentration), full line (left); n-butanol (10^{-6} M), dashed line; hexane (saturated solution of unknown low concentration), dotted line; 10% (w/w) BSA ($5 \cdot 10^{-7}$ M), full line (right). $\Delta\lambda_{SES} = \lambda_{em} - \lambda_{ex} = 12.5$ nm (bandwidths $\Delta\lambda_{em} = \Delta\lambda_{ex} = 5$ nm).

3.2. DiS-C_3(3) fluorescence in cell suspensions and protein solutions

Addition of cells to a diS-C_3(3) solution in Hepes elicited significant changes in its fluorescence. The SES maximum of diS-C_3(3) fluorescence in cell suspensions of increasing cell concentrations was progressively red-shifted, the overall spectrum broadened and intensity increased compared to its fluorescence in pure buffer, evidently due to the occurrence of a new spectral component, as illustrated in Fig. 4.

A similar effect was observed with diS-C_3(3) solutions in PBS containing increasing concentrations of proteins (bovine serum albumin (BSA) or horse serum, pH 7.4). In a solution containing 10% BSA (w/w) and $3 \cdot 10^{-7}$ M dye, the SES maximum was observed to have shifted to $\lambda = 582$ nm, while the SES component seen in pure aqueous solutions at $\lambda < 550$ nm had practically vanished, Fig. 3.

3.3. SES of diS-C_3(3) fluorescence in NaOH solutions

The SES of diS-C_3(3) fluorescence was investigated in concentrated aqueous NaOH (0.5–3 M NaOH) where the cationic dye molecules interact electrostatically with OH^- ions, which interaction might be expected to simulate the effect of dye charge neutralization due to electrostatic interaction with nearby negative charges in its protein binding sites.

With increasing concentrations of NaOH, the SES maximum was continuously and reversibly shifted from 569 nm in pure aqueous solution to 582 nm in 3 M NaOH, and the intensity increased about 4-fold. The spectrum in 3 M NaOH, i.e., F_n, the spectrum of neutral (OH^- ion-paired) diS-C_3(3), was nearly identical to that of bound dye (F_b) in albumin solutions. The SES of diS-C_3(3) in NaOH solutions were therefore analyzed in terms of a linear combination of F_a and F_b components: $F_n = aF_a + bF_b$. The b values obtained were proportional to the concomitant decrease of 'free' charged dye SES intensity a. For measurements made with the RF-540 spectrofluorimeter under the conditions described above, a proportionality factor of 4.1 was obtained.

3.4. DiS-C_3(3) binding to cells and proteins

Using the decomposition of experimental synchronous emission spectra into free and bound dye components, the dependence of bound dye SES intensity in cell suspensions on (i) dye concentration and (ii) cell concentration, was investigated. A typical example of the dependence on dye concentration is shown in Fig. 5 for a suspension of $6 \cdot 10^6$ cells/ml in Hepes containing 5 mM KCl and 10^{-6} M

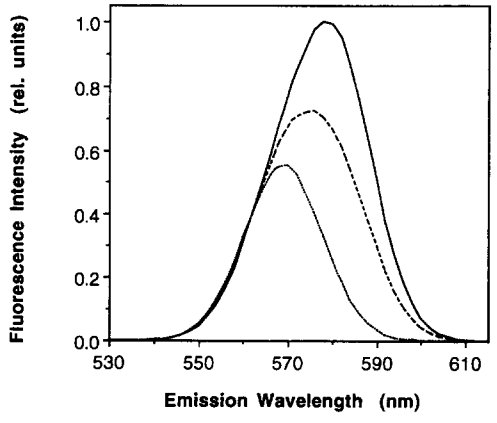

Fig. 4. Dependence of SES spectra of $3.75 \cdot 10^{-8}$ M diS-C_3(3) in suspensions of FDCP-Mix clone A4 cells in Hepes containing 5 mM KCl and $1.5 \cdot 10^{-6}$ M valinomycin (pH 7.4) on the cell concentration: without cells, dotted line; $3 \cdot 10^6$ cells/ml, dashed line; $6 \cdot 10^6$ cells/ml, full line.

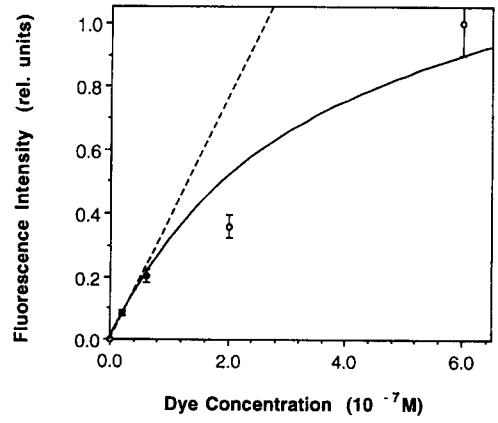

Fig. 5. Dependence of the fluorescence of the bound diS-C_3(3) component (bF_b) on dye concentration: $1 \cdot 10^6$ FDCP-Mix clone A4 cells/ml in Hepes containing 5 mM KCl and $1 \cdot 10^{-6}$ M valinomycin (pH 7.4): circles, experimental data; dotted line, linear fit to the data at low concentration.

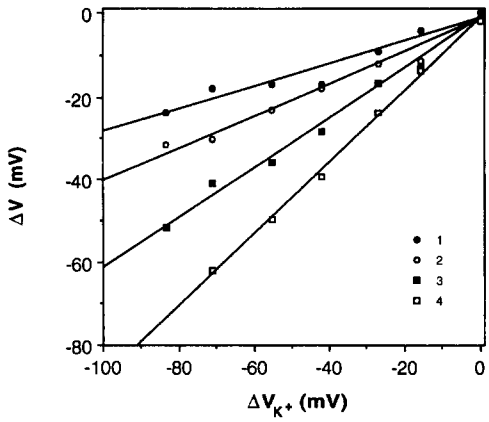

Fig. 6. DiS-$C_3(3)$ fluorescence of suspensions of FDCP-Mix clone A4 cells in Hepes containing 10^{-6} M valinomycin, at pH 7.4, as a function of extracellular potassium concentration, plotted as ΔV versus ΔV_{K^+} (see Results). Data from EPICS V: curve 1 ($6 \cdot 10^6$ cells/ml, $1.25 \cdot 10^{-7}$ M dye), curve 2 ($6 \cdot 10^6$ cells/ml, $3 \cdot 10^{-8}$ M dye). SES spectral analysis: curve 3 ($6 \cdot 10^6$ cells/ml, $1.25 \cdot 10^{-7}$ M dye), curve 4 ($0.4 \cdot 10^6$ cells/ml, $3 \cdot 10^{-8}$ M dye).

valinomycin. The dye concentration was increased from $2 \cdot 10^{-8}$ to $6 \cdot 10^{-7}$ M. A clear indication of saturation can be seen in the curvature for dye concentrations higher than $\approx 5 \cdot 10^{-8}$ M, up to which the dependence is linear. The bound dye SES component for either of these dye concentrations was proportional to the cell concentration over the range used, up to $6 \cdot 10^6$ cells/ml (linear regression coefficients 0.96 to 0.99). A similar proportionality was observed for BSA solutions, at least up to 2% (w/w) albumin. In both cases, the intensity of the bound dye component increased at the expense of that of the free dye. When both dye and cell concentrations in suspensions were increased while keeping their ratio constant, the value of $Q = b/a$ also remained practically constant.

3.5. DiS-$C_3(3)$ fluorescence response to changes in extracellular potassium concentration

In Fig. 6 (curves 3 and 4) the results of the assessment of relative transmembrane potential in cells are presented as ΔV versus ΔV_{K^+}, determined according to Eqs. (5) and (11), respectively. RT/F was taken as 25.6 mV, corresponding to an average temperature of 24°C. These calibration curves represent examples of the results of more than 20 experiments, performed with various cell preparations labelled with either $3 \cdot 10^{-8}$ or $1.25 \cdot 10^{-7}$ M diS-$C_3(3)$. Curves 1 and 2 in Fig. 6 were obtained from flow cytometric determinations, the 'ΔV' ordinate there reflecting, strictly, the logarithmic differences of I_{mean} (i.e., b, proportional to c_{in}) rather than of Q (i.e., b/a, proportional to c_{in}/c_{out}).

Linear calibration curves were well fitted to the experimental data, linear regression coefficients ranging from 0.94 to 0.997 being obtained. Both ΔV and $\ln(I_{mean}/I_{mean130})$ were thus found to be almost exactly proportional to the increment of potassium diffusion potential ΔV_{K^+}, with negligible intercept offset (−0.5 to −1.5 mV). The experimental slopes determined for the different cell preparations ranged from 0.25 ($1.25 \cdot 10^{-7}$ M dye, flow cytometer) to 0.85 ($3 \cdot 10^{-8}$ M dye, SES) and exhibited a well-defined dependence on the dye concentration: the slopes for samples labelled with $1.25 \cdot 10^{-7}$ M diS-$C_3(3)$ (at which concentration the response was beginning to show the effects of saturation, as seen in Fig. 5) were all about 1.5-times smaller than those obtained for the same sample using $3 \cdot 10^{-8}$ M dye (still in the linear response range). However, for a given dye concentration, no systematic differences were observed between slope values measured by spectral analysis of SES and flow-cytometric intensities.

Only a moderate diS-$C_3(3)$ binding to cuvette walls was observed during the course of the calibration procedure (less than 10% over 20 min). Moreover, any possible role of this effect on the assessment of transmembrane potential is alleviated for the SES procedure by the relative nature of that measurement.

4. Discussion

4.1. Origin and analysis of the fluorescence signal

The pronounced changes of diS-$C_3(3)$ SES observed on redistribution of the dye from buffer to cells have a clear parallel in the changes observed upon binding to bovine serum albumin and to the constituents of horse serum. It is therefore reasonable to attribute the cell-induced changes to binding to intracellular proteins. While binding to other cellular macromolecules, such as RNA, can also change diS-$C_3(3)$ spectra in a similar way (data not shown), the much higher protein content, particularly in the cytosol, strongly supports a dominant role for protein dye-binding.

The mechanism of the changes in probe fluorescence is probably related to dye charge neutralization in electrostatic binding of the cationic diS-$C_3(3)$ molecules to negatively-charged binding sites on the proteins. Two observations in particular support this model: (i) a virtually identical change in diS-$C_3(3)$ SES is induced by neutralizing the dye charge in concentrated NaOH solutions, and (ii) diS-$C_3(3)$ fluorescence intensity is very low in cell nuclei which contain a large predominance of histones, positively-charged proteins. The electrostatic interaction of dye molecules with either negative ions (OH^-) or polyions (e.g., acidic proteins) can evidently perturb molecular electronic orbitals, with a concomitant change in molecular absorption and emission characteristics.

The fluorescence quantum yield of protein-bound diS-$C_3(3)$ may also be increased by virtue of the less polar environment of the protein binding site, as suggested by the increases in diS-$C_3(3)$ fluorescence intensity on changing solvent from water to ethanol to n-butanol (Table 1).

The respective role of these two phenomena, however, is unimportant as far as the assessment of transmembrane potential changes is concerned. The quantum yield enters only in the constant P, the value of which it is not necessary to determine.

Using the unique capability of synchronous fluorescence to resolve moderate emission spectral differences, the contributions of free (in solution) and bound (probably mainly to cellular protein) forms of diS-C_3(3) could be determined in cell suspensions in terms of linear combinations of their individual SES. The relevant ratio, $Q = b/a$, of the two components, reflecting the distribution of the probe between cells and the extracellular medium, eliminates possible perturbing variations in dye concentration in the samples, as caused for instance by dye binding to cuvette walls.

As long as the dye binding within cells is proportional to c_{in}, the Q value monitors the Nernstian ratio of unbound dye concentration inside and outside the cells (c_{in}/c_{out}). It does so to within a constant scale factor determined by the relative quantum yields and spectral variations in detection efficiency of the fluorescence of bound dye in the cell (whether partitioned sub-cellularly into mitochondria or not) to those of unbound dye in the external solution. The condition of proportional dye-binding within cells corresponds to concentrations far from saturation, i.e., to the condition that the ratio of concentration of dye bound to that of binding sites (protein) available be small (≈ 0.1 or less). This proviso was checked by measuring the dependence of bF_b in hyperpolarized cells on the extracellular dye concentration. As shown in Fig. 5, for a cell concentration of 10^6 cells/ml effects start to became significant at dye concentrations exceeding $\approx 5 \cdot 10^{-8}$ M above which proportionality between Q values and (c_{in}/c_{out}) is no longer maintained.

4.2. Relative scales for changes in transmembrane potential

The ΔV versus ΔV_{K^+} calibration curves obtained (Fig. 6) demonstrate that the proposed methods, i.e., spectral analysis of SES and flow-cytometric intensities, provide a proper linear scale for estimating transmembrane potential (at least within appropriate ranges of the dye and cell concentrations explored, including even those for which saturation effects are already beginning to become evident). Although the slopes of individual calibration curves obtained were found to vary from one preparation of cell sample to another, and could be different – but not systematically so – for the data based on I_{mean} (i.e., effectively on b alone) obtained with the cytofluorimeter and that for b/a obtained via cuvette measurement of SES, they decreased in the same ratio on increasing the dye concentration for a given cell sample from $3 \cdot 10^{-8}$ M to $1.25 \cdot 10^{-7}$ M (i.e., from well below to well above the onset of saturation effects) for a given preparation. The most likely reason for the variation in slope of the experimental curves under otherwise nominally constant conditions of dye and cell concentration, is that the conductances of the cell plasma membrane for other major ions, which might vary according to the precise history of the cells during and prior to preparation for measurement, are not negligible compared with the high conductance for K^+ expected to be induced by valinomycin. The consequence of this is predictable from the Hodgkin-Horowitz equation (see, e.g., [26,27]), which relates the transmembrane potential V to the major transmembrane ion gradients through their corresponding Nernst equilibrium potentials:

$$V = T_{K^+}V_{K^+} + T_{Na^+}V_{Na^+} + T_{Cl^-}V_{Cl^-} + \Delta V_{act} \quad (15)$$

where T_{K^+}, T_{Na^+}, and T_{Cl^-} are the so-called transport numbers (relative membrane conductances) of potassium, sodium and chloride ions, respectively, and ΔV_{act} the (small) contribution of other active ion pumps to the transmembrane potential, the relative contributions of K^+, Na^+ and Cl^- to the overall potential varying very considerably between different cell types and physiological states. The basic assumption usually invoked in connection with the valinomycin effect is that this K^+-specific ionophore increases the potassium ion conductance to a value well in excess of those of the other ions so that, essentially, $V = V_{K^+}$. Thus, if the valinomycin-induced K^+ conductance does not exceed the other ionic conductances by more than an order of magnitude, the V_{K^+} contribution to the transmembrane potential V might still be dominant, but the slope of the ΔV versus ΔV_{K^+} calibration curve will be reduced from unity to $T_{K^+}/(T_{K^+} + T_{Na^+} + T_{Cl^-})$ if no appreciable changes are induced in the conductances or potentials of any of these ions by the change in external K^+ concentration, resulting in a possibly quite sensitive dependence of the slope on the condition of the cells with respect to regulation of the balance of these physiologically important ions. If, on the other hand, any of the conductances or balances of these major ions is, in fact, appreciably sensitive to the external K^+ concentration, this should be indicated, in general, by observation of a non-linear ΔV versus ΔV_{K^+} relationship, again providing in principle a sensitive test for such changes. Such non-linearity may not be strong over the available range of external potassium ion concentration, and no evidence for such was obtained in the present study. In any event, it seems quite likely that the variation in the slope of the ΔV versus ΔV_{K^+} determinations between separate, nominally identically prepared, samples as well as the non-systematic variations between flow-cytometric and SES determinations on the same samples, reflect physiological differences arising from, possibly quite subtle, variations in the physical and/or chemical environments between samples and between cuvette and flow determinations.

Most importantly, however, such dependences (linear or otherwise) provide the possibility, in principle, of qualitatively detecting and monitoring even quite rapid, physio-

logically relevant changes in the intracellular balance of these major ions brought about by changes in external conditions of both non-specific (temperature, osmotic pressure, pH) and specific (e.g., growth and differentiation factors, both promoting and inhibiting) perturbers of cell state. It should be noted here too, that the applicability of this relative method is not abrogated by differences in the binding capacity of the cell for the fluorophore *as long as both responses are in the linear response range of dye and cell concentrations*, since the binding capacity then only affects the scale factor P (see Eqs. (2) and (4)) which does not appear in the transmembrane potential difference scales ΔV for the different cell states. The practicality of such an approach has been confirmed by more recent data demonstrating just such a difference in the slopes of these ΔV versus ΔV_{K^+} determinations between the FDCP-Mix clone A4 cells used in the investigations reported when grown in presence of the specific growth-factor IL-3 and when deprived of it for a few hours, but still viable (Plášek et al., in preparation).

4.3. Absolute changes in transmembrane potential

The extension of these results to the measurement of transmembrane potential differences between different cell states on an *absolute* (mV) scale by direct comparison of Q values without calibration, using Eq. (5) directly, is more problematical, despite the indirect experimental support adduced above for its theoretical basis. In contrast with the relative method, constancy of the binding capacity of the cytosolic and, where relevant, mitochondrial proteins (and possibly other species), as well as of the fluorescence quantum yield of the probe, is a fundamental requisite for such an absolute comparison. While this assumption is unlikely to be violated when monitoring transmembrane potential following changes in extracellular ion concentration (as is reasonably assumed for the ΔV_{K^+} calibration procedure) or other changes effecting rapid alterations in transmembrane potential, it need not necessarily remain valid following long-term cell physiological changes, when protein and DNA synthesis, mitochondrial activity and/or the structure of the cytoplasm may be expected to be affected. In such cases, the logarithm of relative probe fluorescence intensities will not monitor the true magnitude of the difference in transmembrane potential between the states, and it is then essential to calibrate the probe fluorescence response using one or other (or preferably all) of the various calibration procedures to be found in the literature (e.g., [9,10,13,17]).

With due regard to the last proviso, where necessary, this *absolute* measurement of transmembrane potential, combined with the *relative* measurements (which indirectly reflect differences in major ion transport and balance between the states in question) established in this work as linearly quantitating transmembrane potential changes and discussed above, promises to be useful for indicating real changes in transmembrane potential and their likely origin in realistic biological contexts such as, for example, following the application of specific stimuli rapidly or more slowly affecting cell state or function, as already indicated for the specific growth factor response of the haemopoietic stem-cell line employed in these studies.

4.4. The role of mitochondria

It might have been thought, a priori, that serious difficulties would be likely to arise from the superposition of bound probe signals originating in both cytosol and mitochondria, since the latter are known to exhibit their own characteristic transmembrane potential [24]. While the FDCP-Mix clone A4 cells exploited in this study contain only a few mitochondria, at least less than about a dozen (Lord, B.T., personal communication) with a total volume, based on typical mitochondrial size (e.g., [24]), of only about 2% of that of the cytosol (compared, for instance, with about 5% for mature lymphocytes), their Nernstian accumulation of cationic dye may still result in up to around 20-fold more dye localised therein than in the cytoplasm, due to the very high transmembrane potential (up to -200 mV) of active mitochondria. In fact, as will be reported in detail elsewhere (Plášek et al., in preparation), confocal fluorescence microscopy of individual FDCP-Mix clone A4 cells (Bio-Rad MRC600 with a 60 × Nikon PlanApo immersion objective, 514.5 nm argon-ion laser excitation, observation via rhodamine filter of standard GHS barrier set) revealed a clear fluorescent structure of bright spots, too many to be assignable to the small number of mitochondria, but evidently representing localised regions of high binding capacity for the dye, possibly associated with endoplasmic reticulum [28]. This was superimposed on a relatively uniform dimly fluorescent background in the cytoplasm, the intensity in the nuclei being much lower still, the nuclei taking up the appearance of dark holes in the cytoplasm (peripheral rings, however, typical of fluorescently labelled plasma membranes, were never observed). Whether or not a major fraction of the dye is distributed within mitochondria under the experimental conditions of the measurements of cell states of interest in the presence of valinomycin, the determinations will remain valid (subject to the proviso already indicated) as long as, under these conditions, the mitochondrial transmembrane potential does not differ between the states in question (see Eq. (9) et seq.). In that case, only changes in the *plasma*-membrane transmembrane potential are then indicated by changes in the slope of ΔV versus ΔV_{K^+} and/or by the direct determination of ΔV when valid, albeit predominantly through fluorescence emanating from the mitochondria.

In connection with a definitive demonstration of the role of mitochondria, it should also prove possible to separate the cytoplasmic signal from that due to mitochondria by employing a specific inhibitor of mitochon-

drial activity which abrogates its transmembrane potential [29]. Again, in providing also the opportunity to simultaneously monitor the mitochondrial transmembrane potential directly, the recently developed carbocyanine dye JC-1, which emits bright green fluorescence upon its accumulation in cytosol but orange fluorescence in mitochondria [30], may provide a more elegant and less artifact-prone solution to this problem. Our ongoing investigations are aimed at resolving the question of the role of mitochondria by discrimination of the mitochondrial and plasma-membrane transmembrane potentials using the methodology reported here.

Acknowledgements

The authors wish to express their gratitude for criticisms of the originally submitted text by a reviewer which led them to include a detailed appraisal of the role of mitochondria in the observed phenomena, a presentation of the theoretical near equivalence of fluorimetric measurements on cell suspensions and flow-cytofluorimetric measurements on single cells, as well as to a discussion of the discrepancies observed between them in practice, and to extensive clarification of the text. The above work was largely carried out at the Cancer Research Campaign Paterson Institute for Cancer Research and was also supported in part by Czech Republic Grant Agency grant Nos. 204/93/2224 and 204/93/0704. The authors gratefully acknowledge the help provided by Dr. Grenham Ireland of the Department of Structural Biology, University of Manchester with the confocal microscopy. J.P. wishes also to thank the Paterson Institute for its hospitality and for personal financial support.

References

[1] Loew, L.M. (1991) in New Techniques of Optical Microscopy and Microspectroscopy (Cherry, R.J., ed.), pp. 255–272, Macmillan Press, London.
[2] Smith, J.C. (1990) Biochim. Biophys. Acta 1006, 1–28.
[3] Gross, D. and Loew, L.M. (1989) in Methods in Cell Biology, Vol. 30 (Taylor, D.L. and Wang Y.-L., eds.), pp. 193–218, Academic Press, New York.
[4] Waggoner, A.S. (1979) Annu. Rev. Biophys. Bioeng. 8, 47–68.
[5] Freedman, J.C. and Novak, T.S. (1989) Methods Enzymol. 172, 102–122.
[6] Cohen, L.B. and Salzberg, B.M. (1978) Rev. Physiol. Biochem. Pharmacol. 83, 35–88.
[7] Bashford, C.L. (1981) Biosci. Rept. 1, 183–196.
[8] Sims, J., Waggoner, A.S., Wang, C.-H. and Hoffman, J.F. (1974) Biochemistry 13, 3315–30.
[9] Hladky, B.S. and Rink, T.J. (1976) J. Physiol. 263, 287–319.
[10] Hoffman, J.F. and Laris, P.C. (1974) J. Physiol. 239, 519–552.
[11] Ivkov, V.G., Pechatnikov, V.A. and Ivkova, M.N. (1984) Gen. Physiol. Biophys. 3, 19–30.
[12] Ivkova, M.N., Pechatnikov, V.A. and Ivkov, V.G. (1984) Gen. Physiol. Biophys. 3, 97–117.
[13] Tsien, R.Y. and Hladky, B.S. (1978) J. Membr. Biol. 38, 73–98.
[14] Ehrenberg, B., Montana, V., Wei, M.D., Wuskell, J.P. and Loew, L.M. (1988) Biophys. J. 53, 785–794.
[15] Plášek, J. and Hrouda, V. (1991) Eur. Biophys. J. 19, 183–188.
[16] Peña, A., Uribe, S., Pardo, J.P. and Borbolia, M. (1984) Arch. Biochem. Biophys. 231, 217–225.
[17] Burkhardt, G. (1977) Biochim. Biophys. Acta 468, 227–237.
[18] Johnstone, R.M., Laris, P.C. and Eddy, A.A. (1982) J. Cell. Physiol. 112, 298–301.
[19] Smith, T.C. (1982) J. Cell. Physiol. 112, 302–305.
[20] Spooncer, E., Heyworth, C.M., Dunn, A. and Dexter, T.M. (1986) Differentiation 31, 111–118.
[21] Lloyd, J.B.F. (1971) Nature 231, 64–65.
[22] Vo-Dinh, T. (1978) Anal. Chem. 50, 396–41.
[23] Vo–Dinh, T. (1981) in Modern Fluorescence Spectroscopy (Wehry, E.C., ed.), Vol. 4, pp. 167–192, Plenum Press, New York.
[24] Alberts, B., Bray, D. Lewis, J. Raff, M., Roberts, K. and Watson, J.D. (1986) Molecular Biology of the Cell, 2nd Edn., pp. 316 and 352, Garland, New York.
[25] (1977) CRC Handbook of Chemistry and Physics, 58th Edn. (Weast, R.L. and Astle, M.J., eds.), pp. E56–E58, CRC Press, Boca Raton, FL.
[26] Kotyk, A. and Janáček, K. (1977) Membrane Transport: an Interdisciplinary Approach, pp. 287–288, Plenum Press, New York.
[27] Jaffe, L.F. (1974) J. Theoret. Biol. 48, 11–18.
[28] Quader, H. (1990) Protoplasma 155, 166–175.
[29] Wilson, H.A., Seligman, B.E. and Chused, T.M. (1985) J. Cell. Physiol. 125, 61–71.
[30] Haugland R.P. (1992) Handbook of Fluorescent Probes and Research Chemicals, 5th Edn., Molecular Probes, Eugene, OR.